QUANTIFYING THE ORIENTATION OF THE REINFORCEMENT IN COMPOSITES: FROM MODEL MATERIALS TO BULK NANOCOMPOSITES

Zheling Li[a*], Robert J. Young[a], Ian A. Kinloch[a], Alexander J. Marsden[b], Neil R. Wilson[b]

[a]*School of Materials, University of Mancheter, Oxford Road, Manchester M13 9PL, United Kingdom*
[b]*Department of Physics, University of Warwick, Coventry CV4 7AL, United Kingdom*
**zheling.li@postgrad.manchester.ac.uk*

Keywords: Graphene, Orientation, Raman Spectroscopy, Nanocomposites

Abstract
In this work, polarized Raman spectroscopy has been used to undertake a systematic study upon quantifying the orientation of graphene and its derivative, graphene oxide (GO), in bulk nanocomposites. Highly-aligned basic graphene units made via chemical vapour deposition (CVD) and highly-ordered pyrolytic graphite (HOPG), together with the randomly-aligned glassy carbon have been used as reference materials. It is found that when a polarized laser beam is parallel to the cross-section of the graphene, the Raman band has its strongest/lowest intensity (I) when the polarization is parallel/perpendicular to the plane of the graphene, ideally following a ~cos^4 dependence on angle. Based on this, a theory has been developed to quantify the degree of reinforcement orientation in nanocomposites.

1. Introduction

There has been a rapid development of the application of composites in recent years. Among the key issues in the study of composites, the orientation of the reinforcement is one of the most critical issues, for its significant influence on property both mechanically and functionally. Nowadays, with nanoscale reinforcements such as graphene, carbon nanotubes and clay there is becoming increasing focus upon their high surface areas and high aspect ratios. However with such large aspect ratios, the orientation of reinforcement needs to be carefully characterized, since even small deviations from the expected values will result in poor estimates of final properties. Additionally the nano-dimensions also make it difficult to be characterized.

2. Experimental Section

2.1 Materials

Graphite (Grade 2369) was supplied from Graphexel Ltd. HOPG (43834, 10x10x1mm) and Glassy carbon (42821, 3mm thick, type 1) was purchased from Alfa Aesar. Poly(vinyl alcohol)(PVA) (Mw~89000-98000, 99+% hydrolyzed) was purchased from Sigma Aldrich. Other reagents are analytical grade and used without further purification. Copper foil was purchased from Alfa Aesar (product number 10950, 99.9999% purity, 0.025 mm thick,) which was cleaned in acetone and isopropanol prior to use.

2.2 CVD Graphene Preparation

Graphene was grown via low-pressure chemical vapour deposition (LP-CVD) on cleaned copper foils.[1] The foils were heated from room temperature to 1000 ^{o}C in a tube furnace with one inch quartz worktube under a hydrogen flow of two standard cubic centimetres per minute (sccm), with a resultant pressure of 10^{-2} mbar. The hydrogen flow was maintained constant throughout the growth process. After annealing for 20 minutes at 1000 ^{o}C, 35 sccm of methane was introduced for a further 10 mins. The methane flow rate was reduced to 5 sccm while the sample was cooled to 600^{o}C, after which, the flow was stopped.

2.3 GO Preparation

GO was prepared with a modified Hummers' method.[2, 3] Briefly, 3 g graphite was added to 70 ml concentrated sulphuric acid under stirring at room temperature. Then the mixture system was kept at 0 ^{o}C after 1.5 g sodium nitrate was added. Under stirring, 9 g potassium permanganate was gradually added slowly. The mixture system was place into a 40 ^{o}C water bath for 0.5 h, followed by addition of 140 ml water and kept stirring for another 15 min. Then 20 ml 6 % w/v H_2O_2 and 500 ml water were added subsequently. After being washed with 250 ml 1:10 HCl aqueous solution by repeating centrifuging for 3 times, the mixture was washed with water until neutral for later use.

2.4 GO/Poly(vinyl alcohol) (PVA) Nanocomposites Preparation

GO/PVA nanocomposites were prepared by liquid casting.[4] The 10 wt% PVA aqueous solution were mixed with GO to obtain several dispersions with GO concentration of 1 wt%, 2 wt%, 3 wt% and 5 wt%. Those dispersions were sonicated to obtain homogenous dispersions followed by standing overnight to fully remove the bubbles in it. Then the dispersions were cast onto petri dishes at room temperature for film formation.

2.5 Polarized Raman Spectroscopy

Raman test was conducted using HeNe laser (λ=633 nm) with a laser spot around 2 μm.[5] A Cartesian coordinate system with '*X*', '*Y*' and '*Z*' axis was defined to describe the experimental settings (Fig.1), where samples was tested in two ways.[4] In '*Z*' direction, the propagation of laser is along the *Z* axis, perpendicular to the top surface of sample; In '*X*' direction, sample is settled vertically with the propagation of laser along *X* axis, perpendicular to the cross section. The 'VV' polarization configurations were applied, where the polarization of incident and scattered radiation both are parallel to '*Y*' direction. Raman polarization configuration was fixed and the sample was rotated to different angle θ_X and θ_Z in '*X*' and '*Z*' direction, respectively, in the full range of 90^{o} with a step of 10^{o}. The X_{VV} and Z_{VV} are defined for polarized Raman tests in '*X*' and '*Z*' directions, respectively. For tests in the '*X*' direction, HOPG and CVD graphene were cold mounted with polyester resin, and the cross section was further polished until graphene was exposed.

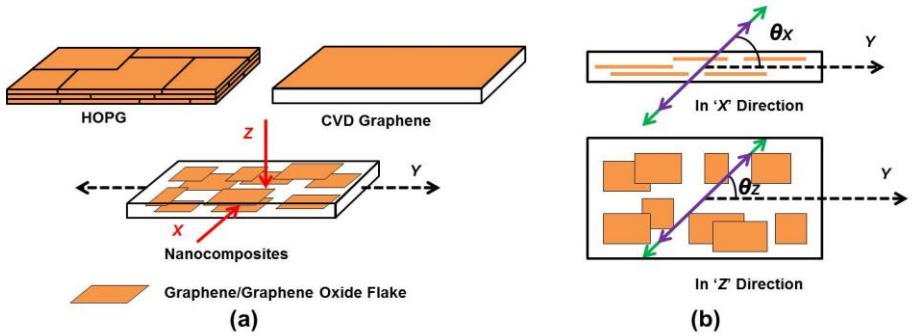

Figure 1. (a) Illustration of Raman spectroscopy test in '*Z*' and '*X*' directions. (b) top view and side view in 'VV' configuration. The red, green and purple arrows represent the direction of laser propagation, incident radiation and scattered radiation, respectively.

3. Result and Discussion

Initially the most commonly used form of graphite – HOPG, with a perfect crystalline graphite structure,[6] was studied. The Raman spectra of HOPG in both '*Z*' and '*X*' directions are shown in (Fig.2(a)). In the spectrum, the Raman G band is located around 1580 cm^{-1}, corresponding to the E_{2g} phonon at the Brillouin zone (BZ) centre (**Γ** point).[7] The strong band around 2650 cm^{-1} called 2D band, also known as G' band, resulted from the two phonons with opposite momentum in the highest optical branch near the **K** point.[8] In the spectrum of X_{VV}, there are the D band around 1300 cm^{-1} and the D' band around 1620 cm^{-1}, originating from inter- and intra-valley scattering at the Brillouin zone boundary,[9] which need to be activated by defects, in this case possibly the discontinuity of the graphene flake in *X* direction. They are absent in Z_{VV} because of the defect-free HOPG basal plane.[10]

The G band intensity (I_G) variation of HOPG in X_{VV} and Z_{VV} are shown in (Fig.2(b)). The intensity has been normalized to the fitted value, respectively. In X_{VV}, I_G varies anisotropically, with the maximum and minimum intensity being at θ_X = 0° and 90°, respectively. In Z_{VV}, I_G keeps constant. Ideally for few-layer graphene with the propagation of laser along its normal, the Raman band intensity exhibits an oscillating behaviour[11, 12] as its edge geometry (zigzag/armchair) changes.[13, 14] While in the basal plane, the band intensity shows no polarization dependence.[14, 15] In mixed composite system with different graphene edge geometries, edges from every direction make a contribution to the Raman band intensity, resulting in an invariant I_G in Z_{VV}.

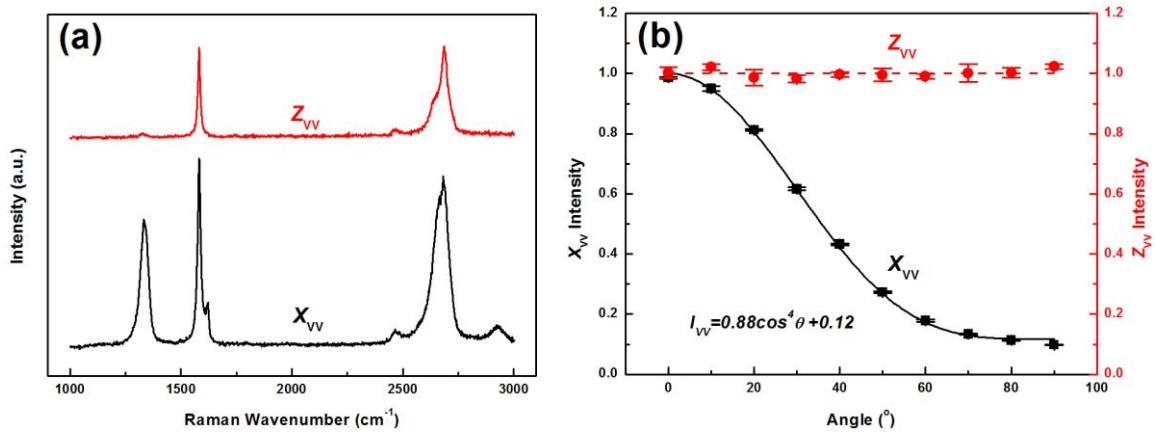

Figure 2. (a) The Raman spectra and (b) I_G variation of HOPG in X_{VV} and Z_{VV}, respectively. The solid lines are the curve fitting using Eq.2 and the dashed line is guide to eyes.

As predicted before,[16, 17, 18] the variation of Raman band intensities with θ_X (defined in Fig.1) for single crystal graphite with a laser beam in the *X* direction (parallel to the graphene planes) with VV polarization should be of the form:

$$I_{VV} \propto \cos^4 \theta_X \quad (1)$$

It can be seen in Fig.2(b) that Eq.1 is not followed strictly, implying the imperfect graphene orientation, possibly resulting from the local wavy structure or debris. It can be modified to give a better fitting by adding the parameters C_1 and C_2 (Eq.2), where $C_1 + C_2$ equals unity. The reason why the parameters are added are due to the fact that the partially oriented graphene would contribute to the integral intensity from all the directions, inconsistent with the original Eq.(1) which relies on premise of perfect oriented graphene. This will be discussed later in detail.

$$I_{VV} \propto C_1 \cos^4 \theta_X + C_2 \quad (2)$$

In the following analysis, the most basic unit – graphene is studied. Fig. 3(a) shows the Raman spectra of the CVD graphene in both X_{VV} and Z_{VV}. In Z_{VV}, the low-intensity D band implies high-quality of the CVD graphene.[8, 19] As the G band for CVD graphene is partially superimposed in the mounting polymer bands, the Raman 2D band intensity (I_{2D}) variation in both X_{VV} and Z_{VV} is used (Fig. 3(b)).

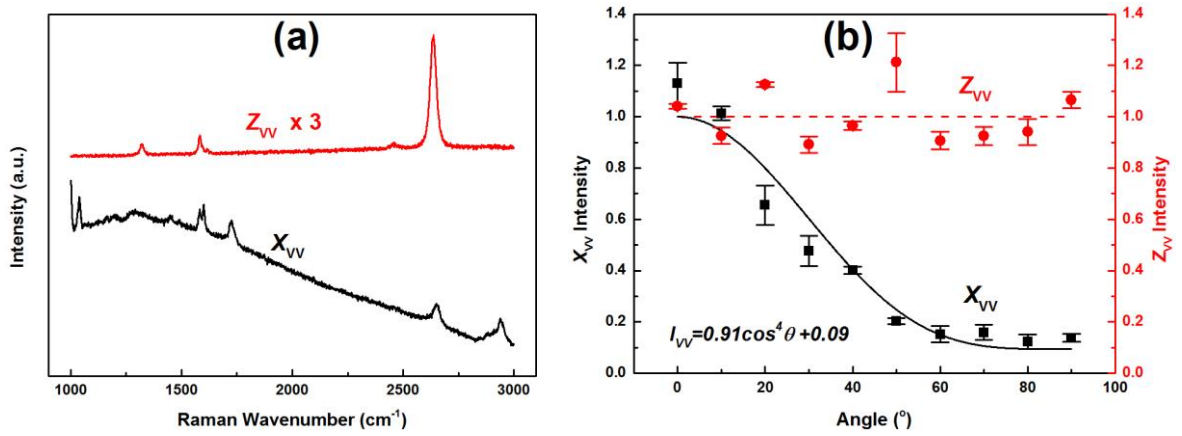

Figure 3. (a) The Raman spectra and (b) I_{2D} variation of CVD graphene in X_{VV} and Z_{VV}, respectively. The solid lines are the curve fitting using Eq.2 and the dashed line is guide to eyes.

The behaviour of the CVD graphene for the different polarization configurations is very similar to that of HOPG. It has a maximum intensity at θ_X = 0° and decreases with θ_X increasing in X_{VV}, with a constant I_{2D} in Z_{VV} being independent of θ_Z again (Fig. 3(b)). The data in X_{VV} has also been fitted using Eq.2, with values of the parameters C_1 and C_2 being similar to those obtained for HOPG.

Beyond these two kinds of graphene materials with well-defined crystalline structure, glassy carbon with a randomly oriented structure[20] was compared as well. Fig.4(a) shows the Raman spectra of glassy carbon in both X_{VV} and Z_{VV}, which has a distinctive D and G band, and a flat 2D band, probably implying isotropy.[20] This has been confirmed by the invariant

I_G in both X_{VV} and Z_{VV} (Fig.4(b)). This is because in glassy carbon, the porous structure leads the graphite flakes to be randomly oriented.[20, 21]

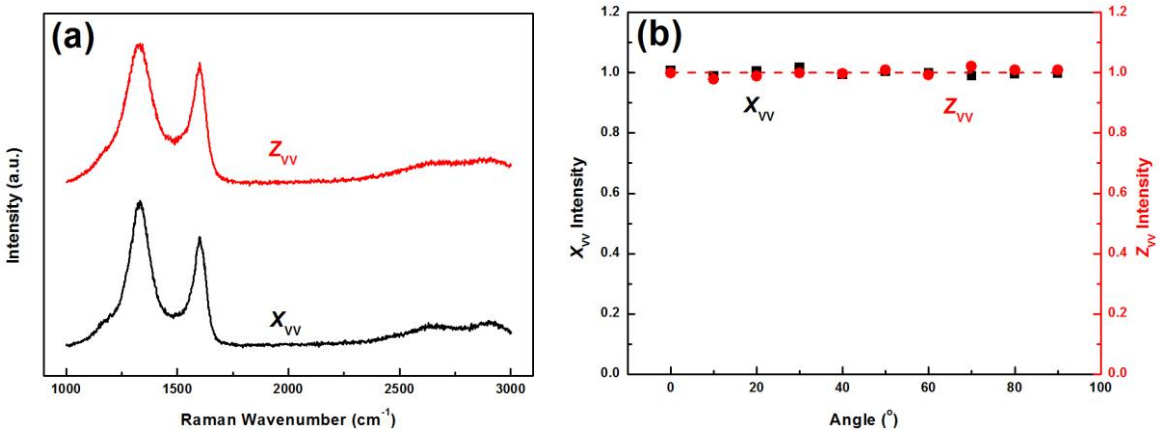

Figure 4. (a) The Raman spectra and (b) I_G variation of glassy carbon in X_{VV} and Z_{VV}, respectively. The dashed lines are guide to eyes.

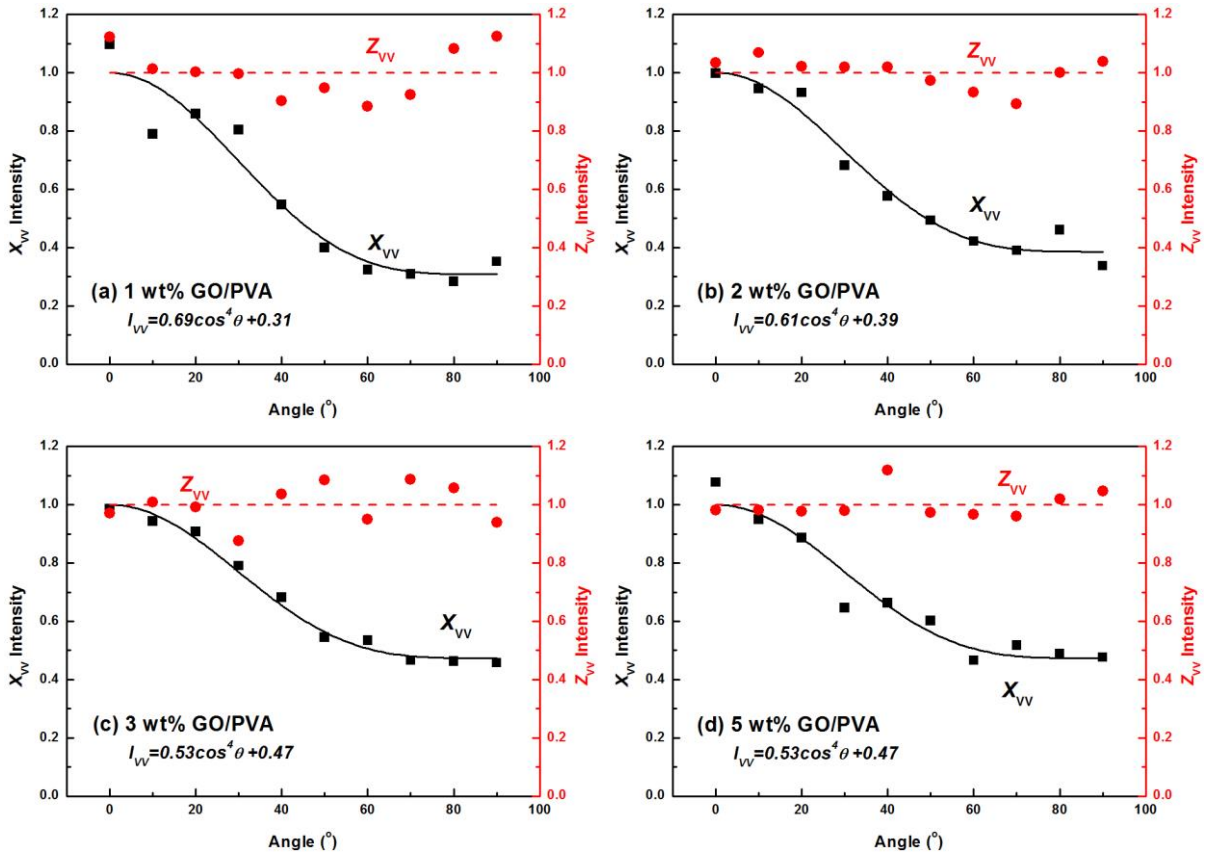

Figure 5. The Raman I_G variation of (a) 1wt% , (b) 2wt% , (c) 3wt% and (d) 5 wt% GO/PVA nanocomposites in X_{VV} and Z_{VV}, respectively. The solid lines are the curve fitting using Eq.2 and the dashed lines are guide to eyes.

The orientation of GO in PVA nanocomposites with different GO loadings was also evaluated using polarized Raman spectroscopy (Fig. 5). It was known from an earlier study[4] that the method of production of the nanocomposite led to the GO flakes being aligned in the plane of the nanocomposite film. Based on I_G variation, it can be seen that the GO flakes are moderately aligned at 1% loading but that their polarization dependence go less significant to

5 % loading. It is thought that the alignment of the GO occurs by settlement at the bottom of the mold during the evaporation of the water solvent. It appears that the settlement for higher loadings of GO does not take place so easily and leads to less well-aligned GO flakes.

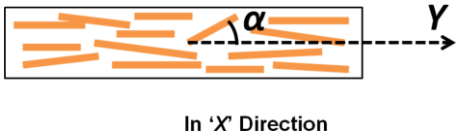

Figure 6. Illustration of the orientation distribution model in the side view. α represents the angle between the GO flakes and *Y* axis, and the definition of others are the same as that in Fig.1.

As mentioned above, the graphene orientation in the materials is by no mean perfect. Some of the graphene are located at an angle to the reference *Y* axis, as shown schematically in Fig.6. In order to predict the graphene orientation and also its effect upon the mechanical properties of a nanocomposite, it is assumed that the variation of the angular orientation of the flakes relative to the *Y* direction takes the form of a Lorentzian distribution, with a probability density function of the form:

$$f(\alpha;0,r) = \frac{1}{\pi}\frac{r}{\tan^2\alpha + r^2}\frac{1}{\cos^2\alpha} \tag{3}$$

where *r* represent the scale parameter ($r \geq 0$), and α represents the variable in angle. It means, graphene appears at all angle in ($-\pi/2$, $\pi/2$,) but with the majority around the *Y* axis. That is the reason why even when the samples are tested at $\theta = 90^o$, there is still weak intensity. Based on this, the Intensity Ratio ψ (where $0 \leq \psi \leq 1$) has been established and correlated with the well-established Krenchel orientation efficiency factor η_o.[22]

As Eq.1 represents the ideal situation and Eq.2 shows the real situation:

$$\text{Intensity Ratio } \psi = \frac{C_2}{C_1 + C_2} = \frac{\int_0^{\frac{\pi}{2}} f(\alpha;0,r)\sin^4\alpha d\alpha}{\int_0^{\frac{\pi}{2}} f(\alpha;0,r)\cos^4\alpha d\alpha} = \frac{r(2r+1)}{r+2}(r \geq 0) \tag{4}$$

The Krenchel orientation efficiency factor[22] is given by an equation of

$$\eta_o = \frac{1}{\pi}\int_{-\frac{\pi}{2}}^{\frac{\pi}{2}} \cos^4\alpha d\alpha \tag{5}$$

Thus it can be given in terms of the intensity ratio ψ as:

$$\eta_o = \frac{2(\sqrt{\psi^2 + 14\psi + 1} + \psi + 7)}{(\sqrt{\psi^2 + 14\psi + 1} + \psi + 3)^2} \tag{6}$$

In this case, for perfectly oriented materials, $C_1 = 1$, $C_2 = 0$, $\psi = 0$ and $\eta_o = 1$; for randomly oriented materials, $C_1 = 0$, $C_2 = 1$, $\psi = 1$ and $\eta_o = 3/8$, thus a constant I_{2D} in X_{VV} will be observed like that in Z direction. This result corresponds to the Krenchel orientation efficiency values calculated before, further confirming its validity in charactering the graphene in either graphene itself or graphene-based nanocomposites.

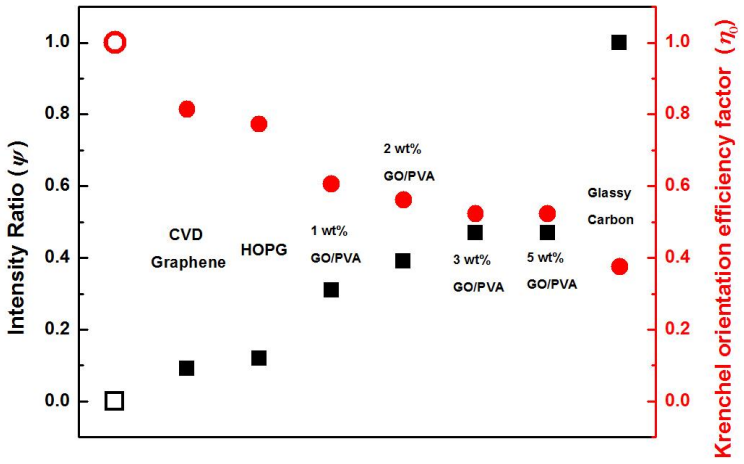

Figure 7. The Intensity Ratio ψ and Krenchel orientation efficiency factor η_o of those graphene-based materials (solid square and circle). The points with perfect orientation is indicated by the open square/circle.

It is shown in Fig.7 that when the graphene-based materials go from model materials to nanocomposites, their Raman intensity ratio keep increasing, together with the decreasing Krenchel orientation efficiency factor until it reaches 3/8, which represents the random graphene orientation, indicating the less graphene orientation. Based on the polarized Raman spectroscopy, the graphene orientation can be quantified and it is envisaged that this theory will be applicable to a wide range of composite systems reinforced with nanoplatelets.

4. Conclusion

Polarized Raman spectroscopy has been used to establish a systematic study upon quantifying the orientation of HOPG, CVD graphene, glassy carbon and graphene-based nanocomposites. It is found that the Raman bands intensity and the angle between laser polarization and graphene follows a function of $I = C_1\cos^4\theta + C_2$. The value of C_2 can be a reflection of the degree of graphene orientation, being higher for a degree of lower orientation, until it reaches 1, which is a character for isotropic materials like glassy carbon. Based on the polarized Raman spectroscopy, the graphene orientation could be quantified and it is envisaged that this theory will be applicable to a wide range of composite systems reinforced with nanoplatelets.

References

[1] N. Wilson, A. Marsden, M. Saghir, C. Bromley, R. Schaub, G. Costantini, T. White, C. Partridge, A. Barinov, P. Dudin, A. Sanchez, J. Mudd, M. Walker and G. Bell. Weak Mismatch Epitaxy and Structural Feedback in Graphene Growth on Copper Foil. *Nano Research*, *6* (*2*): 99-112, 2013.

[2] W. S. Hummers and R. E. Offeman. Preparation of Graphitic Oxide. *J. Am. Chem. Soc.*, *80* (*6*): 1339-1339, 1958.

[3] Y. Xu, K. Sheng, C. Li and G. Shi. Self-Assembled Graphene Hydrogel Via a One-Step Hydrothermal Process. *ACS Nano*, *4* (*7*): 4324-4330, 2010.

[4] Z. Li, R. J. Young and I. A. Kinloch. Interfacial Stress Transfer in Graphene Oxide Nanocomposites. *ACS Applied Materials & Interfaces*, *5* (*2*): 456-463, 2013.

[5] L. Deng, S. J. Eichhorn, C.-C. Kao and R. J. Young. The Effective Young's Modulus of Carbon Nanotubes in Composites. *ACS Applied Materials & Interfaces, 3* (*2)*: 433-440, 2011.

[6] H. Hiura, T. W. Ebbesen, K. Tanigaki and H. Takahashi. Raman Studies of Carbon Nanotubes. *Chem. Phys. Lett., 202* (*6)*: 509-512, 1993.

[7] J. Zabel, R. R. Nair, A. Ott, T. Georgiou, A. K. Geim, K. S. Novoselov and C. Casiraghi. Raman Spectroscopy of Graphene and Bilayer under Biaxial Strain: Bubbles and Balloons. *Nano Lett., 12* (*2)*: 617-621, 2011.

[8] A. C. Ferrari, J. C. Meyer, V. Scardaci, C. Casiraghi, M. Lazzeri, F. Mauri, S. Piscanec, D. Jiang, K. S. Novoselov, S. Roth and A. K. Geim. Raman Spectrum of Graphene and Graphene Layers. *Phys. Rev. Lett., 97* (*18)*: 187401, 2006.

[9] M. Begliarbekov, O. Sul, S. Kalliakos, E.-H. Yang and S. Strauf. Determination of Edge Purity in Bilayer Graphene Using M-Raman Spectroscopy. *Appl. Phys. Lett., 97* (*3)*: 031908-3, 2010.

[10] G. Katagiri, H. Ishida and A. Ishitani. Raman Spectra of Graphite Edge Planes. *Carbon, 26* (*4)*: 565-571, 1988.

[11] K.-i. Sasaki, R. Saito, K. Wakabayashi and T. Enoki. Identifying the Orientation of Edge of Graphene Using G Band Raman Spectra. *J. Phys. Soc. Jpn., 79* (*4)*: 044603, 2010.

[12] C. Cong, T. Yu and H. Wang. Raman Study on the G Mode of Graphene for Determination of Edge Orientation. *ACS Nano, 4* (*6)*: 3175-3180, 2010.

[13] L. G. Cançado, M. A. Pimenta, B. R. A. Neves, M. S. S. Dantas and A. Jorio. Influence of the Atomic Structure on the Raman Spectra of Graphite Edges. *Phys. Rev. Lett., 93* (*24)*: 247401, 2004.

[14] A. K. Gupta, T. J. Russin, H. R. Gutiérrez and P. C. Eklund. Probing Graphene Edges Via Raman Scattering. *ACS Nano, 3* (*1)*: 45-52, 2008.

[15] L. G. Cançado, M. A. Pimenta, B. R. A. Neves, G. Medeiros-Ribeiro, T. Enoki, Y. Kobayashi, K. Takai, K.-i. Fukui, M. S. Dresselhaus, R. Saito and A. Jorio. Anisotropy of the Raman Spectra of Nanographite Ribbons. *Phys. Rev. Lett., 93* (*4)*: 047403, 2004.

[16] P. Tan, C. Hu, J. Dong, W. Shen and B. Zhang. Polarization Properties, High-Order Raman Spectra, and Frequency Asymmetry between Stokes and Anti-Stokes Scattering of Raman Modes in a Graphite Whisker. *Physical Review B, 64* (*21)*: 214301, 2001.

[17] Q. Liang, X. Yao, W. Wang, Y. Liu and C. P. Wong. A Three-Dimensional Vertically Aligned Functionalized Multilayer Graphene Architecture: An Approach for Graphene-Based Thermal Interfacial Materials. *ACS Nano, 5* (*3)*: 2392-2401, 2011.

[18] E. López-Honorato, P. J. Meadows, R. A. Shatwell and P. Xiao. Characterization of the Anisotropy of Pyrolytic Carbon by Raman Spectroscopy. *Carbon, 48* (*3*): 881-890, 2010.

[19] A. W. Robertson and J. H. Warner. Hexagonal Single Crystal Domains of Few-Layer Graphene on Copper Foils. *Nano Lett., 11* (*3)*: 1182-1189, 2011.

[20] G. M. Jenkins and K. Kawamura. Structure of Glassy Carbon. *Nature, 231* (*5299)*: 175-176, 1971.

[21] S. Yamada and H. Sato. Some Physical Properties of Glassy Carbon. *Nature, 193* (*4812)*: 261-262, 1962.

[22] H. Krenchel. *Fibre Reinforcement*. Akademisk Forlag, Copenhagen, 1964.